Slip-controlled thin film dynamics

R. Fetzer[1], M. Rauscher[4], A. Münch[2,3], B. Wagner[2], K. Jacobs[1]

[1] Department of Experimental Physics, Saarland University, 66041 Saarbrücken, Germany
[2] Weierstrass Institute for Applied Analysis and Stochastics, Mohrenstr. 39, 10117 Berlin, Germany
[3] Institute of Mathematics., Humboldt University Berlin, 10099 Berlin, Germany
[4] Max Planck Institute for Metals Research, Heisenbergstraße 3, 70569 Stuttgart, Germany

Abstract

In this study, we present a novel method to assess the slip length and the viscosity of thin films of highly viscous Newtonian liquids. We quantitatively analyse dewetting fronts of low molecular weight polystyrene melts on Octadecyl- (OTS) and Dodecyltrichlorosilane (DTS) polymer brushes. Using a thin film (lubrication) model derived in the limit of large slip lengths, we can extract slip length and viscosity. We study polymer films with thicknesses between 50 nm and 230 nm and various temperatures above the glass transition. We find slip lengths from 100 nm up to 1 μm on OTS and between 300 nm and 10 μm on DTS covered silicon wafers. The slip length decreases with temperature. The obtained values for the viscosity are consistent with independent measurements.

1   Introduction

Miniaturization of chemical appliances into so-called microfluidic devices allows to handle smaller and smaller amounts of liquid. However, in narrow channels, the effect of the hydrodynamic boundary conditions becomes extremely important. In particular, small amounts of slip on the channel walls can improve throughput and decrease the dispersion of chemical signals [19]. In electronics industry, downscaling photolitographic processes requires extremely thin films of photoresist, a polymeric liquid. The dynamics of these thin films is also significantly affected by the boundary condition at the solid/liquid interface. Hence, there is a strong need to quantify slippage of different liquids on various substrates, and to characterise the influence of system parameters on the effective slip length. Common techniques to measure the velocity at the substrate involve tracer particles [1, 2, 11] or fluorescence recovery after photobleaching [16, 9, 17]. In addition, there are various indirect methods to determine the amount of slippage, mostly drainage experiments, e.g., in a surface forces apparatus [3, 22, 23] or between a colloidal probe particle and a wall [4, 20, 7]. For recent reviews see refs. [13, 10]. As none of these techniques can be applied to all liquid/substrate-combinations, we present here an alternative method which is most suited for highly viscous fluids on partially and non-wetting substrates. We use the dewetting process of supported polystyrene (PS) films to induce flow. Slip length and capillary number are then extracted from the shape of the rim around the growing holes in the dewetting film (see for example 1). For determining in addition the viscosity of the liquid with the help of our model, we independently measure the rim velocity.
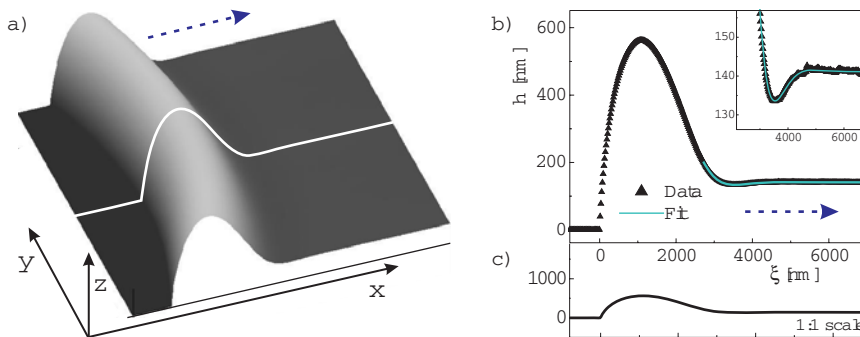
1

Figure 1: Profile of a moving front. a) SPM image of a section of the rim around a hole in a 130 nm thick PS(13.7k) film on OTS at 120°C, scan size 10 μm. The dashed arrow indicates the direction of rim motion. b) A cross section taken in radial direction (white line in the left image) gives the rim profile (triangles) which is well fitted by an exponentially decaying oscillation (solid line). The inset shows an enlarged view of the oscillation. c) Data of b in 1:1 scale.

2   Experiments

The liquids we used in our experiments were atactic polystyrene (PS) melts with molecular weight 5.61 kg/mol, 13.7 kg/mol, and 18 kg/mol (each $M_n/M_w = 1.06$, PSS Mainz, Germany). We prepared polymer films with thickness 50(3) nm, 130(5) nm, and 230(5) nm by spin casting from a toluene solution onto mica, floating on Millipore water, and picking up by hydrophobised Si wafers (Wacker, Burghausen, RMS roughness 0.1 nm). We used standard techniques to hydrophobise wafers with self assembled Octadecyl- and Dodecyltrichlorosilane (OTS and DTS) monolayers [21]. The receding contact angle of PS droplets on OTS as well as on DTS covered Si wafers is 67(3)°.

After heating the films above their glass transition temperature (about 100°C) dewetting takes place. Holes nucleate, grow, and coalesce until in the later stage of dewetting only a set of droplets remain on the substrate. During the early stage of this process, we measured the radii of the radial growing circular holes, R, as a function of time with optical microscopy to determine the dewetting velocity. Once the holes had reached a radius of about 12 μm, we immediately quenched our samples to room temperature to bring the samples in the glassy state. Using scanning probe microscopy (SPM Multimode, Digital Instruments, Santa Barbara, USA) in Tapping Mode^{TM} we measured the glassy rim profiles. To ensure that the rim does not change its shape while cooling we also scanned liquid profiles, but could not detect any difference in shape.

3   Thin film analysis

Flow of thin Newtonian liquid films with no or weak slip at the substrate is well described by the thin film equation as discussed in detail, e.g., in ref. [14]. The essence of the underlying lubrication approximation is the assumption that the lateral scale of thickness variations in the film L is large as compared to the characteristic film thickness H (in this paper the thickness of the undisturbed film). In the linear Navier slip model, the amount of slip at the solid/liquid interface is characterised by the slip length b. The boundary condition for the velocity component parallel to the substrate is $u = b\partial u/\partial z$. Recently, a thin film model has been developed for the case where the slip length is much larger than the film thickness scale H [5, 8, 12]. Neglecting inertia, the lateral velocity in the film for this model is given by

$$u = \frac{2\,b}{h}\,\partial_x\left(2\,\eta\,h\,\partial_x u\right) + \frac{b\,h}{\eta}\partial_x\left(\sigma\,\partial_x^2 h\right), \tag{1}$$

with the viscosity η and the surface tension γ. In eq. (1), we neglect the influence of the disjoining pressure that arises due to the long-range intermolecular forces which drive the dewetting, since we only study regions of the film with a minimum thickness of about 50 nm. However, these forces can be easily included in the model [12]. The first term on the right side is proportional to the divergence of the total longitudinal shear stress integrated over the film thickness. The second term is the gradient of the Laplace pressure. The dynamics of the film thickness induced by the flow is then obtained from the continuity equation

$$\partial_t h + \partial_x(h\,u) = 0. \tag{2}$$

In order to analyse the decay of the rim profile close to the undisturbed film of thickness H, see inset to fig. 1b, we linearise eqs. (1) and (2) about the undisturbed state of thickness $h = H$ and $u = 0$ by introducing a small perturbation $\delta h(x,t) = h(x,t) - H$ and a small velocity $u(x,t)$. The resulting linear equation for $\delta h(x,t)$ is equivalent to the Newtonian limit of the model used in ref. [6] to investigate the rim shape of viscoelastic dewetting films.

We assume that the shape change of the rim due to accumulation of liquid during hole growth is slow as compared to the relaxation time for $\delta h(x,t)$ and $u(x,t)$. The experimental observation indeed shows that dewetting is much faster than the growth of the rim. Then, in a frame of reference $\xi = x - s(t)$ comoving with the position of the rim $s(t)$ we have a quasi-stationary profile. We solve the linear equation with the normal modes ansatz $\delta h = \delta h_0 \exp\{\kappa\xi\}$ and $u = u_0 \exp\{\kappa\xi\}$, and get the following characteristic equation for κ

$$(H\,\kappa)^3 + 4\,\mathrm{Ca}\,(H\,\kappa)^2 - \mathrm{Ca}\,\frac{H}{b} = 0, \tag{3}$$

with the capillary number $\mathrm{Ca} = \frac{\eta\,\dot{s}}{\sigma}$ and the speed of the rim $\dot{s} = \partial_t s$. eq. (3) is a
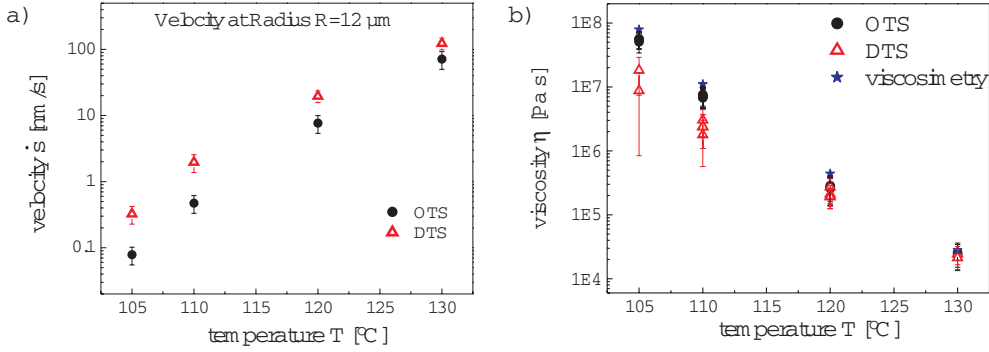
Figure 2: a) Rim velocity of holes with a radius of 12 μm in 130 nm thick PS(13.7k) films dewetting from OTS and DTS covered silicon wafers as a function of temperature. The velocities were measured by optical microscopy. Note the logarithmic velocity scale. b) Viscosity as a function of temperature extracted from rim profiles of 130 nm thick PS(13.7k) films which dewet from OTS and DTS. As expected, the obtained values for the viscosity are identical on both substrates and in good agreement with independent viscosimetry data.

polynomial of third order and has therefore three solutions, one of which is real and positive and therefore unphysical. For $\text{Ca}^2 < 3^3 H/(4^4 b)$, i.e., for slowly dewetting films or for moderately large slip length, the remaining two solutions are a complex conjugate pair $\kappa = \kappa_r \pm i\kappa_i$ with $\kappa_r < 0$. In this case, the rim is expected to have an oscillatory shape as shown in fig. 1. In fact, even for small slip lengths (where the model used here is not valid) rim shapes are always oscillatory, in particular in the no-slip case [18]. For rapidly growing holes or large slip lengths both remaining solutions κ_1 and κ_2 are real and negative, which allows rims to decay monotonically. The aforementioned inequality also implies that the transition in the rim shapes can occur even for fixed b, if the film thickness H is changed; increasing H has the same effect as decreasing b (with the other quantity held fixed).

With scanning probe microscopy (SPM) we measured the rim shape of dewetting liquid PS(13.7k) films of 130 nm thickness on hydrophobised Si wafers (for details see section "Experiments"). We also repeated some experiments with thinner (50 nm) and thicker (230 nm) films, and longer (18k) as well as shorter (5.61k) chain lengths. Depending on the type of substrate coating, densely grafted Octadecyl- (OTS) or Dodecyltrichlorosilane (DTS) polymer brushes, and on the dewetting temperature, we observed oscillatory or monotonically decaying profiles. The observed contact angles of polystyrene droplets which are left on DTS and OTS after the dewetting process are both 67(3)°, yet the rim velocities on DTS are much larger than on OTS, cf. fig. 2a), indicating a difference in slip length. We like to emphasize, however, that the method we develop here for determining the slip length does not depend on the contact angle.

As demonstrated in fig. 1 for the case of an oscillatory profile, an exponentially damped oscillation $\delta h_{osci} = \delta h_0 \exp(\kappa_r \xi) \cos(\kappa_i \xi + \phi)$ (fit parameters are δh_0, κ_i, κ_r,

and ϕ) captures the decay towards the resting film thickness in the experimental data very well. From the fit we gain the inverse decay length κ_r and the wave number κ_i, and from independent measurements we know the surface tension σ and the film thickness H. Inserting $\kappa = \kappa_r \pm i\kappa_i$ into eq. (3) and separating real and imaginary part we get two linear equations for the two unknowns Ca and b, which can easily be solved.

In the case of monotonically decaying rims, we fit the data with a superposition of two exponentials $\delta h_{mono} = \delta h_1 \exp(\kappa_1 \xi) + \delta h_2 \exp(\kappa_2 \xi)$ (fit parameters $\delta h_{1/2}$ and $\kappa_{1/2}$) with inverse decay lengths κ_1 and κ_2. Both, κ_1 and κ_2, fulfill eq. (3) such that we again get a simple system of two linear equations for Ca and b.

Additionally, we can determine the film viscosity η from the capillary number Ca, using the surface tension $\sigma = 30.8$ mN/m and the observed dewetting velocity $\dot{s}$. We like to emphasize that in order to determine solely the slip length, the knowledge of both the dewetting velocity and the viscosity is not required.

4 Results

In order to test the consistency of our method, we performed experiments with films of various thicknesses, and we analysed the rim shapes of the same film at different times, i.e., at different hole sizes and therefore at different rim velocities. The values for the viscosity should only depend on temperature and on chain length, whereas the slip length can additionally depend on the type of substrate.

Fig. 2b) shows the results for the viscosity gained from qualitatively very different profiles of 130 nm thick films on OTS (oscillatory) and DTS (monotonic). They are in very good agreement. Additionally, they are in accordance with the values obtained in a viscosimeter. (The scatter over almost an order of magnitude is not unusual for viscosity values.)

We repeated single experiments with PS films of 50 nm and 230 nm thickness on both types of substrate and obtained identical values for the viscosity and the slip length. Qualitative comparison of the corresponding rims demonstrates that it is possible to induce a transition between an oscillatory shape and a monotonic decay by solely changing the initial film thickness H: as predicted, we observe that thicker films tend to more pronounced oscillations, whereas on thinner films oscillations are suppressed.

We also analysed rim profiles of holes at different dewetting stages, as shown in fig. 3. As the radius R of a hole grows, dewetting slows down due to the growing rim. As predicted, a decrease in rim velocity results in a more pronounced oscillatory shape. Thus, the rim changes its shape while growing (see also ref. [12]). Nevertheless, the slip length extracted from these profiles remains constant within the error bars, i.e., it is independent of the velocity (see fig. 3b). We also verified that the same is true for the estimates of the viscosity obtained from the capillary number, i.e., we found
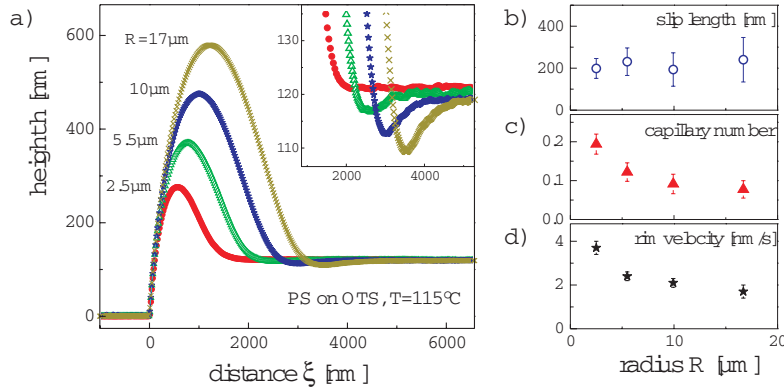
5

Figure 3: Rim analysis at different dewetting stages. a) Cross section of in situ SPM scans of the rim around a hole at radii 2.5 μm (filled circles), 5.5 μm (open triangles), 10 μm (stars), and 17 μm (crosses) (i.e., at different times) in a 130 nm thick PS(13.7k) film on OTS at 115°C. Between $R = 2.5$ μm and $R = 5.5$ μm we observe a transition from monotonic to oscillatory rim shape (see the enlarged view in the inset). b) Slip length and c) capillary number determined from the profiles shown in a). While the capillary number decreases by over a factor of two, the slip length stays constant. d) Rim velocity as determined independently.

that the values for Ca that resulted from the fit of the profiles are proportional to the rim velocity, cf. fig. 3c) and 3d).

Above we checked the consistency of our method and state that it yields reliable values for the viscosity and the slip length. We can now proceed and analyse the dependence of the slip length on temperature and substrate type. The results are summarised in fig. 4a). We find that on OTS slippage is reduced by about one order of magnitude as compared to DTS. This result is in agreement with the observed dewetting velocities: Holes grow significantly faster on the DTS brush. Additionally, on both types of coating, the slip length decreases with increasing temperature, as does the viscosity.

The question arises whether b can be written as a function of η, e.g., as $b = \eta/k$ with a temperature-independent friction coefficient k. The Navier slip condition is often written in terms of this proportionality factor k between slip velocity and shear stress at the substrate. To answer this, we repeated some experiments with PS(5.61k) and PS(18k), henceforth changing the viscosity at constant temperature. All samples had chain lengths below the entanglement length in order to exclude viscoelastic effects. As expected, the viscosity we gain from the rim profiles increases with molecular weight. Plotting the slip length of all samples versus the corresponding viscosity (see fig. 4b) we can collapse the data onto two master curves, one for OTS and one for DTS. The dependence, however, is clearly non-linear. Indeed, the DTS data is nicely fitted by a power law $b \sim \eta^q$ with exponent $q = 1/2$. This corresponds to a friction coefficient k that increases with viscosity. On OTS, the data for high viscosity values can be fitted by the same power law, but for small values of η the
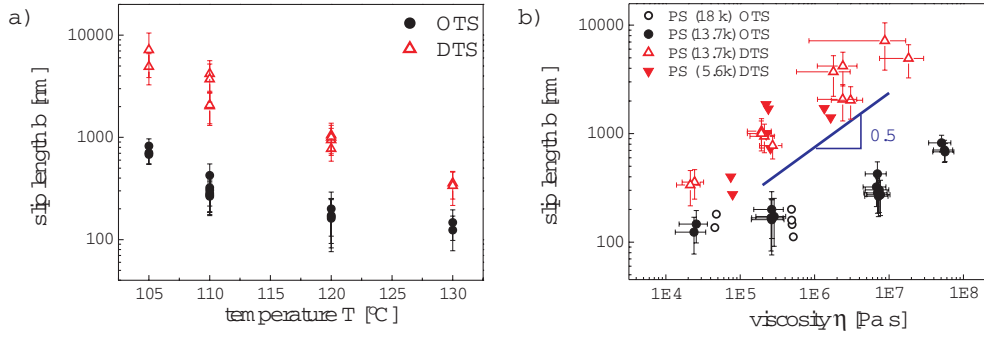
6

Figure 4: a) Slip length of polystyrene films on OTS and DTS as a function of temperature. The values are determined via eq. (3) from the rim profiles of 130 nm thick PS(13.7k) films. b) Slip length of all investigated films plotted against their respective viscosity. Since the data collapse onto two curves, one for OTS (circles) and one for DTS substrates (triangles), b can be written as function of η. The solid line marks a slope of 0.5, indicating that the DTS data is better fitted by $b \sim \eta^{1/2}$ rather than a linear dependence. The OTS data does not follow a power law.

slip length increases only slightly with the viscosity.

5   Summary and discussion

We analysed the profiles of rims around holes in thin dewetting Newtonian PS films on OTS and DTS covered silicon wafers. To capture the form of the profile, we used a thin film model in the strong slip regime. Fitting the theoretical functions to the experimental data, we gained the capillary number and the slip length. Additional knowledge of the dewetting velocity allowed the extraction of the viscosity of the liquid via the capillary number. Analysing profiles of films of different molecular weight, we found that the slip length on the short brush (DTS) is significantly larger than on the long brush (OTS), leading to higher dewetting velocities on DTS as compared to OTS. We moreover observed that the slip length is a non-linear monotonically increasing function of the viscosity. On DTS, the slip length increases roughly with the square root of the viscosity. Furthermore, the data shown in fig. 4b) indicate that the chain length of the polymer molecules seems to play no significant role for the amount of slippage. This is in accordance with the expectation for polymer melts below the entanglement length.

Our finding, that the friction coefficient k is a monotonically increasing function of the viscosity indicates that the mechanism for the momentum transfer between the liquid and the solid and the microscopic origin of the viscosity are related. Since the viscosity decreases with temperature, the friction coefficient must also decrease with temperature. Recent molecular dynamics simulations show that the anchoring of a polymer melt on a brush decreases with decreasing penetration of the melt into the

brush [15]. Moreover, the penetration was found to be lower for smaller melt density. Unfortunately, all simulations were performed at the same temperature such that we can only speculate about the influence of temperature on the anchoring. But since our brushes are quite short and densely packed, we do not expect large changes in the brush structure over the temperature range covered in our experiments, but the melt density decreases slightly, probably enough to explain our findings. However, this must remain a speculation unless further corroborated by experiments and simulations.

Another speculation concerns the origin of the different slip lengths on the two types of brushes. The OTS and DTS brushes might have slightly different properties, e.g., not exactly identical density or short-ranged interaction forces, which give rise to a different anchoring density of the polymer onto the brush. We have, however, no insight in the molecular motion of the fluid particles near the wall, since we analysed the film surfaces and used continuum theory based on hydrodynamics. Hence, we cannot give any prediction about the molecular mechanism that leads to the observed slip length. Here we see a playground for further experimental investigations, probably involving scattering techniques to gain insight into the details of anchoring.

To conclude, we have developed a new consistent method to determine the slip length as well as the viscosity of dewetting thin films based on Newtonian hydrodynamics. This powerful tool now offers the potential to quantify slippage in comprehensive studies using various substrates and liquids. It is now possible to systematically investigate the influence of system parameters, e.g., substrate roughness, viscosity, and even viscoelasticity. To explain the latter, we may note that our current model only applies directly to Newtonian liquids. Highly viscous fluids, in particular polymeric liquids, often exhibit viscoelastic behaviour, i.e., the fluid has an internal time constant τ for the relaxation of stresses generated by shear. However, these viscoelastic properties are only relevant if the Weissenberg number $Wi = \tau\dot{\gamma}$, i.e., the product between the relaxation time and the shear rate is of order one or larger. Thus our Newtonian model remains valid for viscoelastic fluids, if they move slowly enough. A model that captures viscoelastic effects is currently under way.

Acknowledgements

References

[1] Tretheway D. C. and Meinhart C. D. Apparent fluid slip at hydrophobic microchannel walls. Phys. Fluids, 14:L9, 2002.

[2] Tretheway D. C. and Meinhart C. D. A generating mechanism for apparent fluid slip in hydrophobic microchannels. Phys. Fluids, 16:1509, 2004.

[3] Baudry J. Crassous J.-Restagno F. Cottin-Bizonne C., Jurine S. and Charlaix É. Nanorheology: An investigation of the boundary condition at hydrophobic and hydrophilic interfaces. Eur. Phys. J. E, 9:47, 2002.

[4] Neto C. Craig V. S. J. and Williams D. R. M. Shear-dependent boundary slip in an aqueous newtonian liquid. Phys. Rev. Lett., 87:054504, 2001.

[5] Münch A. Wagner B. A. Fetzer R., Jacobs K. and Witelski T. P. New slip regimes and the shape of dewetting thin films. Phys. Rev. Lett., 95:127801, 2005.

[6] Seemann R. Herminghaus S. and Jacobs K. Generic morphologies of viscoelastic dewetting fronts. Phys. Rev. Lett., 89:056101, 2002.

[7] Vinogradova O. I. and Yakubov G. E. Dynamic effects on force measurements. 2. lubrication and the atomic force microscope. Langmuir, 19:1227, 2003.

[8] Sharma A. Kargupta K. and Khanna R. Instability, dynamics and morphology of thin slipping films. Langmuir, 20:244, 2004.

[9] Léger L. Friction mechanisms and interfacial slip at fluid-solid interfaces. J. Phys.: Condens. Matter, 15:S19, 2003.

[10] Brenner M. P. Lauga E. and Stone H. A. *The no-slip boundary condition.* 2005.

[11] Gansen A. Feuillebois F. Rädler L. O. Lumma D., Best A. and Vinogradova O. I. Flow profile near a wall measured by double-focus fluorescence cross-correlation. Phys. Rev. E, 67:056313, 2003.

[12] Wagner B. A. Münch A. and Witelski T. P. Lubrication models with small to large slip lengths. J.Eng. Math., 53:359, 2005.

[13] Bonaccurso E. Butt H.-J. Neto C., Evans D. R. and Craig V. S. J. Boundary slip in newtonian liquids: a review of experimental studies. Rep. Prog. Phys., 68:2859, 2005.

[14] Davis S. H. Oron A. and Bankoff S. G. Long-scale evolution of thin liquid films. Rev. Mod. Phys., 69:931, 1997.

[15] Müller M. Pastorino C., Kreer T. and Binder K. Static and dynamic properties of the interface between a polymer brush and a melt of identical chains. cond-mat/0510068.

[16] Hervet H. Pit R. and Léger L. Direct experimental evidence of slip in hexade-cane: Solid interfaces. Phys. Rev. Lett., 85:980, 2000.

[17] Hervet H. Schmatko T. and Léger L. Friction and slip at simple fluid-solid interfaces: The roles of the molecular shape and the solid-liquid. Phys. Rev. Lett., 94:244501, 2005.

[18] Herminghaus S. Seemann R. and Jacobs K. Shape of a liquid front upon dewet-ting. Phys. Rev. Lett., 87:196101, 2001.

[19] Tice J. D. Song H. and Ismagilov R. F. A microfluidic system for controlling reaction networks in time. Angew. Chem. Int. Ed., 42:768, 2003.

[20] Yakubov G. E. Vinogradova O. I., Butt H.-J. and Feuillebois F. Dynamic effects on force measurements. i. viscous drag on the atomic force microscope cantilever. Rev. Sci. Instrum., 71:2330, 2001.

[21] Tao S. R. Y.-T. Wassermann S. R. and Whitesides G. M. 1989.

[22] Zhu Y. and Granick S. Limits of the hydrodynamic no-slip boundary condition. Phys. Rev. Lett., 88:106102, 2002.

[23] Zhu Y. and Granick S. No-slip boundary condition switches to partial slip when fluid contains surfactant. Langmuir, 18:10058, 2002.